BBA - Molecular Basis of Disease 1865 (2019) 115–125

Contents lists available at ScienceDirect

BBA - Molecular Basis of Disease

journal homepage: www.elsevier.com/locate/bbadis

SREBP-2 aggravates breast cancer associated osteolysis by promoting osteoclastogenesis and breast cancer metastasis

Zhiwei Jie[a,b,1], Ziang Xie[a,b,1], Wenbin Xu[a,b,1], Xiangde Zhao[a,b], Gu Jin[c], Xuewu Sun[a,b], Bao Huang[a,b], Pan Tang[d], Gangliang Wang[a,b], Shuying Shen[a,b], An Qin[e,*], Shunwu Fan[a,*]

[a] Department of Orthopaedics, Sir Run Run Shaw Hospital, School of Medicine, Zhejiang University, Hangzhou 310016, China
[b] Key Laboratory of Musculoskeletal System Degeneration and Regeneration Translational Research of Zhejiang Province, Hangzhou 310016, China
[c] Department of Bone and Soft Tissue Surgery, Zhejiang Cancer Hospital, Hangzhou 310022, China
[d] Department of Orthopedic, Zhejiang University Huzhou Hospital, Huzhou 313003, China
[e] Department of Orthopaedics, Shanghai Key Laboratory of Orthopaedic Implant, Shanghai Ninth People's Hospital, Shanghai Jiaotong University School of Medicine, Shanghai 200011, China

ARTICLE INFO

Keywords:
SREBP-2
Osteoclast
Breast cancer
Osteolysis
Therapy

ABSTRACT

Bone is one of the most common sites of breast cancer metastasis and a major cause of high mortality in these patients. Thus, further understanding the molecular mechanisms regulating breast cancer-induced osteolysis is critical for the development of more effective treatments. In this study, we demonstrated that important roles sterol regulatory element-binding protein 2 (SREBP-2) play in osteoclast formation a function, and in breast cancer metastasis. SREBP-2 expression was found to be induced during the early stages of osteoclast formation under the control of the RANKL/cAMP-response element binding protein (CREB) signaling cascade. SREBP-2 is subsequently translocated into the nucleus where it participates with other transcriptional factors to induce the expression of NFATc1 required for mature osteoclast formation. Additionally, SREBP-2 was also found to be highly expressed in breast cancer tissues and correlated with a poor prognosis. SREBP-2 was similarly under the transcriptional control of CREB and its induction regulates the expression of matrix metalloproteinases (MMPs), key degradative enzymes involved in bone metastases by breast cancer cells. Accordingly, targeting of SREBP-2 with Fatostatin which specifically inhibits SCAP (SREBP cleavage-activating protein) and prevents SREBP activation, attenuated breast cancer-induced osteolysis *in vivo*. Collectively, our results suggest that SREBP-2 plays a critical role in regulating osteoclastogenesis and contributes to breast cancer-induced osteolysis. Thus, SREBP-2 inhibition is a potential therapeutic approach for breast cancer patients with osteolytic bone lesions.

1. Introduction

The skeleton is one of the key metastatic target tissue for many types of tumors [1]. Almost 80% of breast cancer patients with advanced malignancy show bone metastases, leading to pathological fractures, hypercalcemia, intolerable bone pain, and a series of bone-related deficiencies that seriously impact their quality of life [2]. Bone destruction caused by tumor metastasis is a complex process [3] with excessive activation of osteoclasts the crucial element in tumor-induced osteolysis [4]. Breast cancer cells secretes a number of growth factors including receptor activator of nuclear factor-κB ligand (RANKL) that potently promotes osteoclast formation and activation, resulting in excessive bone resorption [5,6]. The resulting cancer cell-induced bone destruction leads to the release of cytokines from the bone matrix which in turn enhances breast cancer cell proliferation and survival, thus forming a vicious cycle of positive induction [7,8]. Hence, agents that can inhibit both osteoclasts and breast cancer cells, such as bisphosphonates have been shown to be effective for treating breast cancer-induced bone diseases [9,10]. However, the high dose and frequent usage of bisphosphonates have been shown to be associated with serious side effects including non-classical bone fractures and osteonecrosis [11]. Thus, it is imperative that newer novel compounds and molecular targets are identified for the safe and effective treatment of breast cancer-induced osteolysis.

Binding of RANKL secreted from breast cancer cells to its cognate receptor RANK, on the surface of osteoclast precursor cells, leads to the recruitment of TRAF6 and consequently activates various downstream effector pathways including NF-κB and MAPKs (Erk1/2, p38, and JNK).

* Corresponding authors.
E-mail addresses: dr_qinan@163.com (A. Qin), 0099203@zju.edu.cn (S. Fan).
[1] These authors contributed equally to this work.

https://doi.org/10.1016/j.bbadis.2018.10.026
Received 2 July 2018; Received in revised form 22 October 2018; Accepted 23 October 2018
Available online 28 October 2018
0925-4439/

These pathways culminate in the induction of key osteoclast transcriptional factor NFATc1 [12,13]. NFATc1 is considered the terminal switch that regulates osteoclast differentiation by promoting the expression of numerous osteoclast-specific genes involved in osteoclast fusion such as dendritic cell-specific transmembrane protein (DC-STAMP), V-ATPase V0 domain subunit d2 (ATP6V0d2), and bone resorption such as tartrate-resistant alkaline phosphatase (TRAP), and cathepsin K (CTSK) [14,15].

Sterol regulatory element-binding protein 2 (SREBP-2) has been studied extensively in the context of cholesterol homeostasis by transcriptionally regulating the expression of target genes. These include gene for the low-density lipoprotein receptor (LDLR), 3-hydroxy-3-methyl-glutaryl-coenzyme A (HMG-CoA) synthase and HMG-CoA reductase, which are involved in regulating fatty acid and cholesterol synthesis [16]. Interestingly, recent genome-wide DNase-Seq analysis identified SREBP-2 as a novel transcriptional regulator involved in osteoclast differentiation [17]. In addition, the SREBP inhibitor, Fatostatin, has been reported to prevent RANKL-induced bone loss by suppressing osteoclast differentiation [18]. Furthermore, SREBP inhibition was recently found to exert multiple anti-tumor effects in various tumors [19–21]. However, the underlying mechanism by which SREBP-2 regulates osteoclast differentiation and the role of SREBP-2 in breast cancer remains ill-defined.

In this study, we showed that SREBP-2 is induced in a RANKL-CREB dependent pathway and plays a positive role in the regulation of osteoclast formation. SREBP-2 was found to transcriptionally control the expression of NFATc1 by binding to SRE in the promoter of NFATc1. In addition, we found elevated expression of SREBP-2 in breast cancer tissue samples, and the high SREBP-2 expression was positively correlated with invasive breast carcinomas and predictor of poor prognosis. Targeted inhibition of SREBP-2 exerts anti-migration and anti-invasion effects on breast cancer cells *in vitro* and protected against breast cancer-induced osteolysis *in vivo*. Thus, SREBP-2 represents a novel molecular target for the development of specific therapeutic agents for the treatment of osteolytic bone lesions induced by breast cancer metastases.

2. Materials and methods

2.1. Ethics

The animal experiments in this study were approved by the Ethics Committee of Sir Run Run Shaw Hospital, Zhejiang University School of Medicine and performed in accordance with the principles and procedures of the National Institutes of Health (NIH) Guide for the Care and Use of Laboratory Animals and the Guidelines for Animal Treatment of Sir Run Run Shaw Hospital.

2.2. Clinical samples

Slices of formalin-fixed and paraffin-embedded breast cancer tumor tissues and adjacent non-tumor tissues of 6 patients were obtained from Zhejiang Cancer Hospital (China) in accordance with the Chinese National Ethical Guidelines, 'Code for Proper Secondary Use of Human Tissue' (Chinese Federation of Medical Scientific Societies). Written informed consent was obtained from each patient before commencing this study. Patient details and pathomorphological classification of breast cancer tumor are shown in Supplementary Materials and Methods.

2.3. Materials and reagents

Detailed information on the materials, reagents, kits and antibodies used in this study can be found in the Supplementary Materials and Methods.

2.4. Cell culture

Primary bone marrow monocytes/macrophages (BMMs) were isolated from the whole bone marrow of 6-week-old male C57BL/6 mice as described previously [22]. In brief, bone marrow from the femoral and tibial bone, and the isolated BMMs were cultured in α-MEM supplemented with 10% FBS, 100 U/ml penicillin/streptomycin (complete α-MEM) and 30 ng/ml M-CSF. The human breast cancer cell line MDA-MB-231 was a kind gift from Dr. Linbo Wang (Sir Run Run Shaw Hospital, Zhejiang University) and was cultured in DMEM with 10% FBS. All cells were maintained in a humidified atmosphere of 95% air/5% CO_2 at 37 °C and media were changed every other day. All cell lines were tested and were free from mycoplasma.

2.5. In vitro osteoclastogenesis assay

BMMs were seeded into 96-well plates at a density of 8×10^3 cells/well, in quadruplicates, in the presence of 30 ng/ml M-CSF and were allowed to adhere overnight. The next day 50 ng/ml RANKL was added to each well to initiate osteoclastogenesis. Culture medium was replenished with fresh media containing M-CSF and RANKL every second day. After 7 days of culture, cells were gently washed with PBS, fixed in 4% paraformaldehyde for 20 min, and stained for TRAP activity. TRAP-positive cells containing 5 or more nuclei were scored as mature osteoclasts and their cell spread area was measured.

2.6. RNA extraction and quantitative PCR analysis

Total RNA was isolated from cultured cells using the RNeasy Mini Kit (QIAGEN, Valencia, CA, USA) in accordance with manufacturer's protocol. Complementary DNA (cDNA) was synthesized using 1 μg of RNA from each sample, 2 μl of 5× PrimeScript RT Master Mix (Takara Bio, Otsu, Japan), and 4 μl of RNase-free ddH_2O in a total volume of 10 μl. Real-time PCR was performed using an ABI Prism 7500 System (Applied Biosystems, Foster City, CA, USA) with SsoFast EvaGreen Supermix (Bio-Rad, Hercules, CA, USA). Primer sets used and cycling conditions are described in Supplementary Materials and Methods.

2.7. Western blot analysis

Total cellular protein was extracted from cultured cells using RIPA lysis buffer (Sigma-Aldrich) containing complete protease inhibitor cocktail. Lysates were centrifuged at 12,000*g* for 15 min at 4 °C and the supernatants were collected and protein concentration was quantified using BCA in accordance with manufacturer's protocol. Proteins were resolved on 10% SDS-PAGE gels and separated proteins were transferred to polyvinylidene difluoride (PVDF) membranes (Bio-Rad, Hercules, CA, USA). Membranes were blocked in 5% (w/v) skim milk in TBST [50 mM Tris, pH 7.6; 150 mM NaCl; and 0.1% Tween-20] at room temperature for 1 h and then incubated with primary antibodies diluted in TBST containing 1% (w/v) skim milk overnight at 4 °C. After three washes with TBST, membranes were incubated for 1 h at room temperature with the appropriate HRP-conjugated secondary antibodies. Antibody-protein reactivity were visualized using LAS-4000 Science Imaging System following exposure to an ECL substrate (Fujifilm, Tokyo, Japan) and the obtained images were analyzed using ImageJ software.

2.8. Bone resorption assay

BMMs stimulated with RANKL to form osteoclasts over 3 days, were gently removed with cell dissociation buffer and equal numbers of BMM-derived pre-osteoclasts were seeded onto bovine bone discs in triplicates, and maintained for additional 3 days. At the end of the culture period, cells were removed by mechanical agitation and sonication, and resorption pits were visualized an imaged using a FEI

Quanta 250 scanning electron microscope. The resorbed area was quantified using ImageJ software (NIH).

2.9. SiRNA transfection and viral transduction

Transfection of small interfering RNAs specifically targeting SREBP-2 and viral transduction of 3xFLAG-SREBP-2 overexpression were performed in accordance with the manufacturer's protocol. Detailed methods are provided in the Supplementary Materials and Methods.

2.10. Chromatin immunoprecipitation (ChIP) assays

Cellular lysates were extracted and ChIP assays were performed using the SimpleChIP Chromatin IP Kit (Cell Signaling Technology #9002) in accordance with manufacturer's protocol. In brief, BMMs treated with or without RANKL for 48 h were fixed with 1% formaldehyde for 10 min at 37 °C to crosslink proteins to DNA, washed with ice-cold phosphate-buffed saline (PBS) and then lysed with ice-cold PBS containing protease inhibitor cocktail. The following lysis samples were sonicated to shear DNA and cell debris removed by centrifugation. Chromatin was then fragmented by partial digestion with Micrococcal Nuclease to obtain chromatin fragments of 1 to 5 nucleosomes. Fragmented chromatins were then subjected to overnight immunoprecipitation at 4 °C with specific antibodies against SREBP-2 or control IgG. Immuoprecipitates were then incubated with ChIP-grade protein G agarose beads for 2 h at 4 °C with rotation. After several low and high salt washes, reversal of protein-DNA cross-links was carried out and the resulting DNA was purified using DNA purification spin columns. Purified DNA was subjected to PCR. The primers sets are provided in the Supplementary Materials and Methods.

2.11. Transwell cell invasion and migration assay

Transwell cell culture chambers were used to evaluate invasion and migration ability of MDA-MB-231 breast cancer cells as described previously [23]. To evaluate the invasive abilities of cells, the membranes of upper chamber inserts were coated with Matrigel Basement Membrane Matrix (100 μg/cm^2) for 6 h at 37 °C. A total of 5×10^4 MDA-MB-231 cells in 100 μl of serum-free DMEM were seeded onto the Matrigel (invasion assay) or directly onto the membrane (migration assay) of the upper chamber inserts. Then 700 μl of DMEM supplemented with 10% FBS were added to the lower chambers. After incubation for 24 h at 37 °C, migrated cells were washed twice with PBS, fixed with 100% methanol and stained with 3% crystal violet for 15 min at room temperature. Cells that did not migrate and adhered to the upper surface of the membrane were carefully removed using cotton swabs. Cells that migrated through the membrane and into the lower compartment were imaged in five randomly selected fields at 20× magnification under a light microscopy. Quantification of the number of migrated/invaded cells in treatment groups were expressed relative to untreated control using Image J software.

2.12. Intratibial mouse model of breast cancer-induced osteolysis

The intratibial murine model of breast cancer previously established in our lab [24] was used to examine the effect of SREBP-2 inhibition on breast cancer-induced osteolysis. In brief, 100 μl of MDA-MB-231 cells at a final cell density of 1×10^6 cells/ml in PBS were injected directly into the tibiae plateau of BALB/c nu/nu mice (6–8 weeks old, female) *via* a percutaneous approach. Mice were then randomly assigned to one of 3 groups (6 mice per group) and intraperitoneally injected with either PBS (sham control), low dose Fatostatin (10 mg/kg) or high dose Fatostatin (15 mg/kg). Injection was repeated every other day for total of 28 days before the animals were sacrificed. No fatalities were observed after tumor cell implantation or drug administration, and the mice maintained regular activity throughout the duration of the experiment. After sacrifice, the tibiae of all mice were removed and processed for high resolution micro-CT analyses and then histologic examinations.

2.13. Micro-CT scanning

The resected tibiae were fixed and analyzed using the Skyscan 1072 high-resolution μCT scanner (Bruker, USA). Image acquisition was conducted at a voltage of 70 kV, an electric current of 80 μA and an isometric resolution of 9 μm. After reconstruction, a square region of interest set at 0.5 mm from the tibia growth plate, was selected for further qualitative and quantitative analysis. Trabecular bone volume/tissue volume (BV/TV), mean trabecular number (Tb.N), and mean trabecular spacing (Tb.Sp) were measured for each sample.

2.14. Bone histomorphometry and immunohistochemical analysis

Histomorphometry analysis was performed as previously described [22,25]. The tibiae were decalcified in 10% EDTA for 4 weeks and then embedded in paraffin for thin tissue sectioning. Histological sections were prepared for TRAP, hematoxylin and eosin (H&E), and SREBP-2 staining. Tissue sections were analyzed on a Leica DM4000B clinical microscope (Leica Microsystems Wetzlar GmbH, Germany) and analyzed using BIOQUANT OSTEO software (2017 V17.2.60). The percentage of tumor area, TRAP-positive multinucleated osteoclasts and SREBP-2 positive cells normalized to the total area, bone surface area and total cells respectively.

2.15. Statistical analysis

Data presented as mean ± standard error of the mean (SEM) from at least 3 independent experiments. Statistical analyses were performed using GraphPad Prism 6 software (San Diego, CA, USA). Statistical differences were assessed by Student's *t*-test or one-way ANOVA followed by Tukey's post hoc analysis where appropriate. Kaplan–Meier analysis of tumor patients and the log-rank test were performed for comparison of the survival curves according to the SREBP-2 level. *p*-Values < 0.05 were considered significant.

3. Results

3.1. SREBP-2 positively regulates osteoclast formation in vitro

We first examined the gene expression of SREBP-2 during RANKL-mediated osteoclast differentiation. RNA extracted from BMMs treated with M-CSF and RANKL for 0, 1, 3, or 5 days were subjected to PCR analysis. As shown in Fig. 1A, SREBP-2 gene expression was significantly upregulated in a time-dependent manner during osteoclast differentiation. On the other hand, the gene expression of SREBP-1 was ubiquitously expressed but at much lower levels. Next we examined the protein expression and subcellular localization of SREBP-2 during osteoclast formation by Western blot analyses (Fig. 1B) and immunofluorescence microscopy respectively (Supplemental Fig. 1A). Consistent with gene expression, both the precursor (P) and active (N) forms of SREBP-2 protein were upregulated during RANKL-induced osteoclast formation (Fig. 1B) with the active (N) form exhibiting nuclear time-dependent nuclear localization following RANKL stimulation. Interestingly, the expression pattern of the active form of SREBP-2 appears to precede the induction NFATc1, the master transcriptional activator of osteoclast formation (Fig. 1B). In line with its expression pattern suggestive of a role in osteoclast formation, gene knockdown of SREBP-2 significantly inhibited the osteoclast formation both in terms of the total number and size of TRAP-positive multinucleated osteoclasts (Fig. 1C) and this was associated with marked reduction in expression of osteoclast marker genes NFATc1, DC-STAMP, TRAP and cathepsin K (CTSK) (Supplemental Fig. 1C–F). This inhibitory effect of

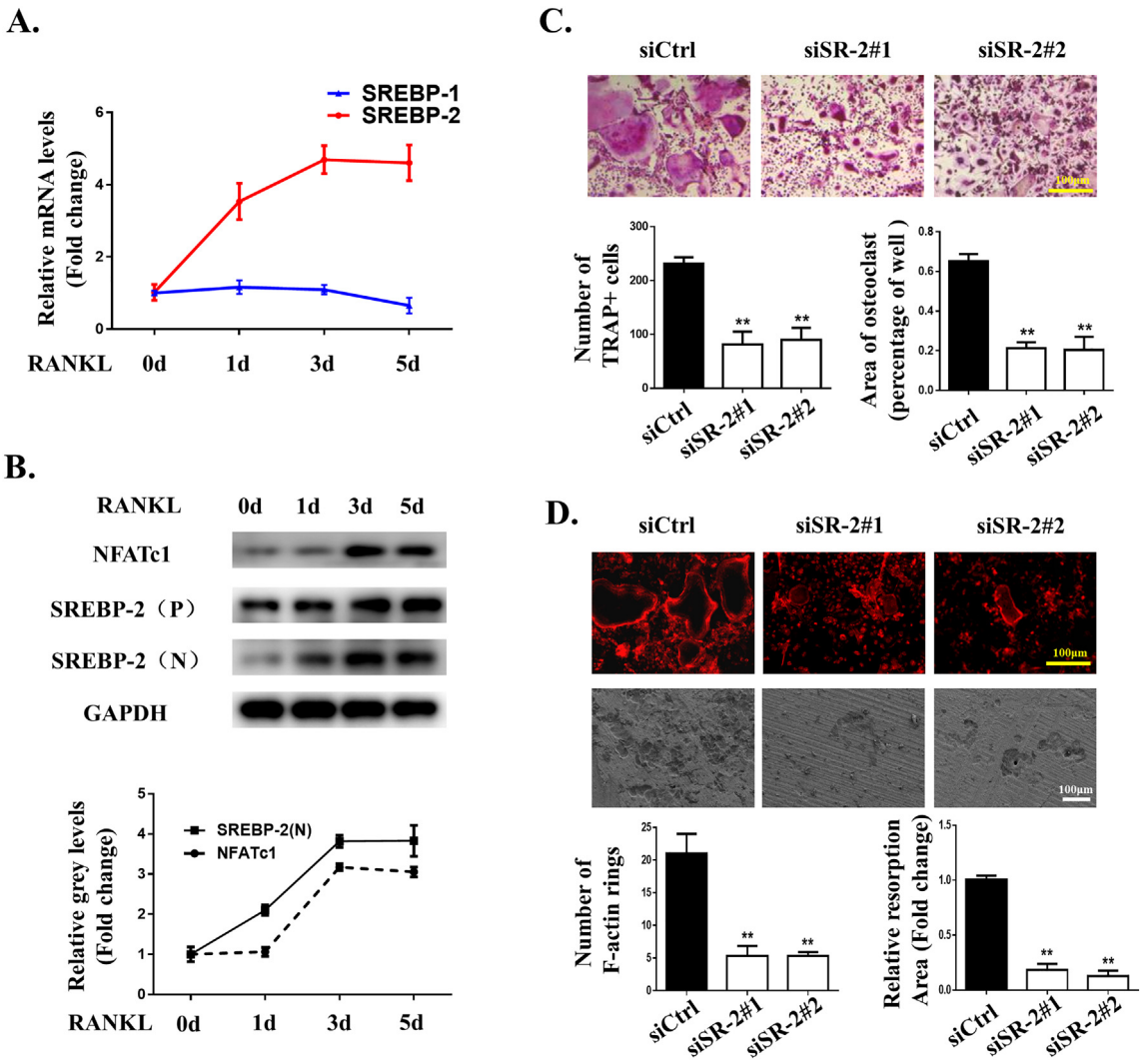

Fig. 1. SREBP-2 positively regulates osteoclast formation and bone resorption *in vitro*. (A) SREBP-1 and SREBP-2 gene expression in BMMs treated with RANKL for 0, 1, 3, or 5 days. $*p < 0.05$, $**p < 0.01$ ($n = 6$). (B) Protein expression of the inactive precursor form of SREBP-2 (P), the active (N) form and NFATc1 in BMMs after treatment with RANKL for 0, 1, 3, or 5 days ($n = 3$). GAPDH was used as internal loading control. (C) BMMs were transfected with SREBP-2 siRNAs (siSR-2#1 or siSR-2#2) or negative scrambled control, after which the cells were stimulated with RANKL for 5 days. At the end of the experimental period, cells were fixed and stained for TRAP activity. The number and area of TRAP-positive multinuclear cells with > 5 nuclei were quantified. $*p < 0.05$, $**p < 0.01$ ($n = 3$). (D) F-actin ring formation and bone-resorption pit analysis were conducted using fluorescence microscopy and scanning electron microscopy, respectively, following siRNA transfection as described above. Three days after stimulation with RANKL, pre-osteoclasts were gently removed and reseeded onto bovine bone discs for examination of bone resorption. The number of F-actin rings and relative resorption area were quantified. $*p < 0.05$, $**p < 0.01$ ($n = 3$). Data are shown as the mean ± s.d. Scale bar, 100 μm.

SREBP-2 knockdown on osteoclast formation and gene expression further translated to inhibitory effect on F-actin ring formation and bone resorption (Fig. 1D). Furthermore, the use of Fatostatin a specific inhibitor of SCAP (SREBP cleavage-activating protein) and prevents SREBP activation, mimics the inhibitory effects of SREBP-2 gene knockdown on osteoclast marker gene expression (Supplemental Fig. 1C–F) providing further evidence of a positive role for SREBP-2 during osteoclast formation *in vitro*.

3.2. SREBP-2 promotes osteoclastogenesis in part by inducing NFATc1 expression

Consistent with a reduction in gene expression, SREBP-2 gene knockdown significantly reduced the protein expression of NFATc1 (Fig. 2A). Similarly Fatostatin treatment potently inhibited the formation of TRAP-positive multinucleated osteoclasts (Fig. 2B) and suppressed the induction of NFATc1 at both the gene (Fig. 2C) and protein levels (Fig. 2D). These inhibitory effects of Fatostatin was partially reversed with overexpression of SERBP-2 (Fig. 2B–D). Taken together, these data suggests that SREBP-2 positively regulates osteoclast differentiation in part by inducing NFATc1 expression.

3.3. SREBP-2 expression is regulated via the RANKL/CREB signaling pathway

We next investigated the underlying mechanisms responsible for the induction of SREBP-2 expression following RANKL stimulation. As shown in Fig. 3A, the level of CREB and activated CREB (*p*-CREB) was time-dependently increased over the 12 h period. Furthermore, the expression and activation of CREB preceded the induction of active SREBP-2 suggesting that RANKL-induced CREB signaling may be involved in the induction of SREBP-2 expression during osteoclastogenesis. Confirming our hypothesis, CREB gene knockdown significantly reduced the expression of active (N) SREBP-2 and NFATc1 (Fig. 3B and Supplemental Fig. 2A–C). Furthermore, treatment of BMMs with KG-501, a potent inhibitor of CREB activity, markedly reduced the

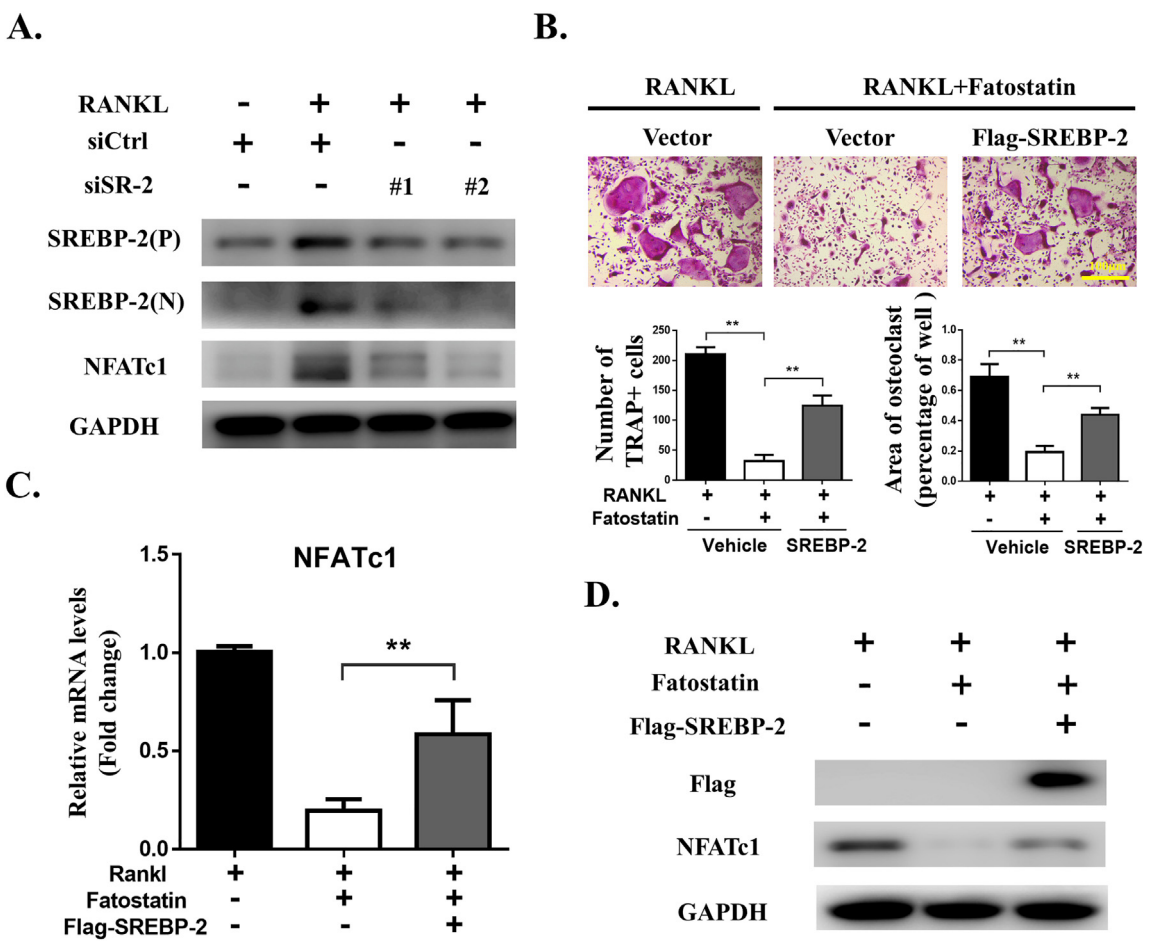

Fig. 2. SREBP-2 regulates NFATc1 expression during osteoclastogenesis. (A) Total cellular proteins extracted from BMMs transfected with SREBP-2 siRNAs or negative scrambled control, and stimulated with RANKL for 5 days were subjected to Western blot analysis using specific antibodies against SREBP-2 (N and P forms) and NFATc1. GAPDH was used as internal loading control. ($n = 3$). (B) BMM cells overexpressing FLAG-SREBP-2 or empty vector were treated with Fatostatin for 5 days for the formation of mature multinucleated osteoclasts. At the end of the experimental period, cells were fixed and stained for TRAP activity. The number and size (area) of TRAP-positive multinuclear cells with > 5 nuclei were quantified. $*p < 0.05$, $**p < 0.01$ ($n = 3$). (C) Real-time quantitative PCR analysis of NFATc1 gene expression using RNA extracted from cells that underwent same treatment in B. $*p < 0.05$, $**p < 0.01$ ($n = 6$). (D) Western blot analysis of protein expression of NFATc1 using total cellular proteins extracted from cells that underwent same treatment as in B. GAPDH was used as internal loading control. ($n = 3$). Data are shown as the mean ± s.d. Scale bar, 100 μm.

formation of TRAP-positive multinucleated osteoclasts (Fig. 3C). Overexpression of SREBP-2 restored osteoclast formation and NFATc1 expression following KG-501 treatment (Fig. 3C and D).

3.4. SREBP-2 regulates the transcription of NFATc1 during osteoclast formation

Using the predictive service at Gene-Cloud of Biotechnology Information (GCBI; https://www.gcbi.com.cn) we generated a transcriptional regulatory network for NFATc1 and identified numerous transcriptional factors including SREBP-2 that were predicted to regulate the NFATc1 gene expression (Fig. 4A). To further analyze the transcriptional regulation of NFATc1 gene by SREBP-2 during osteoclastogenesis we employed transcription element search software (JASPAR; http://jaspar.genereg.net) to screen for putative SREBP-2 binding sites within the 2kB NFATc1 promoter. As shown in Fig. 4B, 5 putative SRE binding sites were identified. To determine whether SREBP-2 can bind to these putative SRE binding sites in the 2kB NFATc1 promoter, we performed ChIP assays. As shown in Fig. 4C and in the absence of RANKL stimulation, we observed basal binding of SREBP-2 to the four of the identified SRE sites. In the presence of RANKL SREBP-2 binding to the SRE sites were dramatically increased consistent with the fact that NFATc1 is a RANKL responsive gene. Furthermore, when in the presence of Fatostatin or KG-501, RANKL-induced binding of SREBP-2 to NFATc1 promoter was attenuated (Fig. 4D) providing further evidence that SREBP-2 is a direct transcriptional regulator of NFATc1 gene expression. Based on these results, we devised a schematic diagram of the role of SREBP-2 in the transactivation of the NFATc1 promoter during RANKL-induced osteoclastogenesis (Fig. 4E).

3.5. SREBP-2 expression predicts poor prognosis in breast cancer patients

Having now established the role for SREBP-2 in osteoclast formation and bone resorption, we next investigated the role of SREBP-2 in breast cancer. We first performed immunohistochemical analysis to examine the expression of SREBP-2 in human breast cancer tissues and adjacent tissues. As we can see in Fig. 5A and Supplemental Fig. 3A, SREBP-2 was highly expressed in breast cancer cells localizing mainly to the nucleus of these cells with the percentage of cells staining positive for SREBP-2 being significantly higher than in adjacent tissues. Furthermore, we performed data mining and analyzed SREBP-2 expression using the publicly available Oncomine platform and TCGA database. The gene expression datasets acquired from the TCGA databases showed that SREBP-2 expression was significantly higher in invasive breast carcinoma than in normal breast tissue which is indicative of a

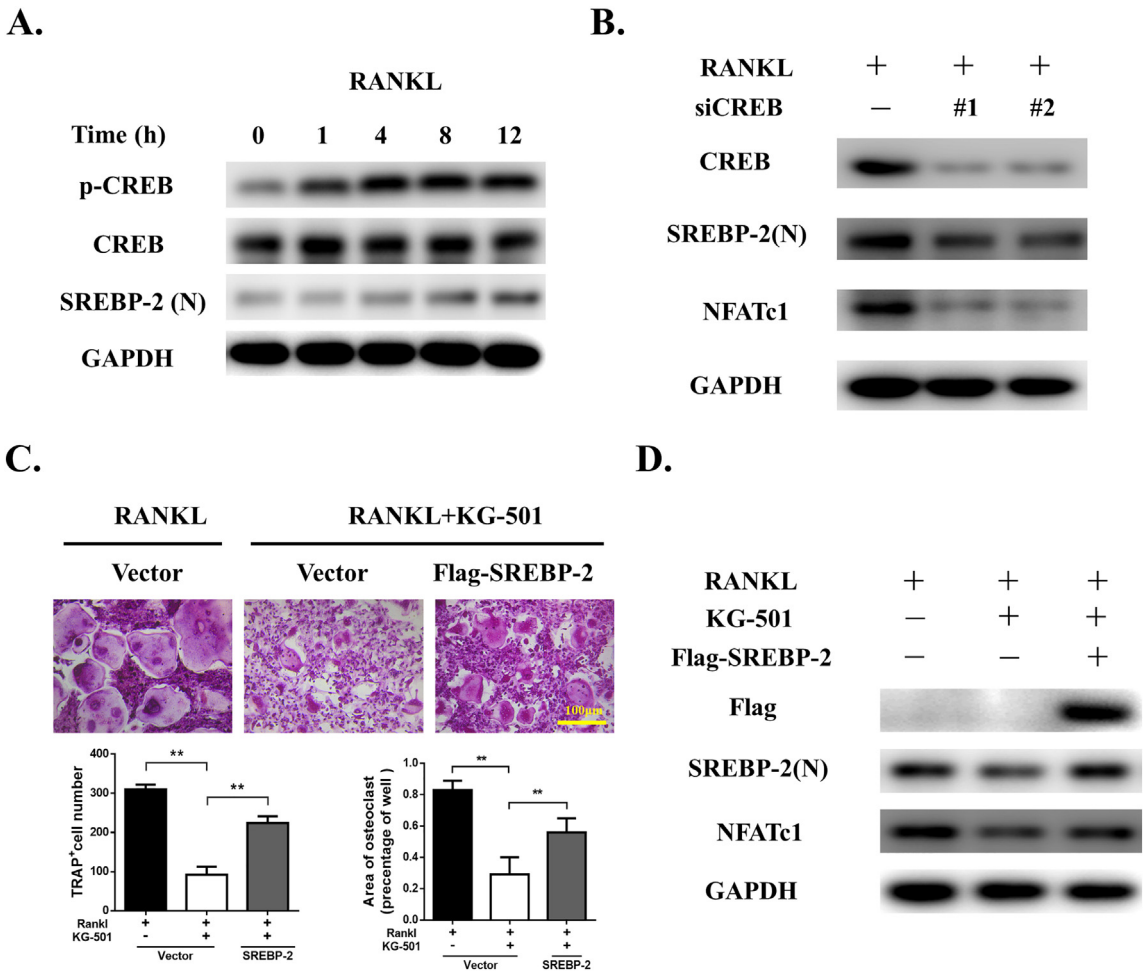

Fig. 3. SREBP-2 expression is induced *via* RANKL/CREB-dependent signaling pathway. (A) Total cellular proteins extracted from BMMs stimulated with RANKL for 0, 1, 4, 8, and 12 h were subjected to Western blot analysis using specific antibodies against SREBP-2 (N form), CREB and phosphorylated CREB (*p*-CREB). GAPDH was used as internal loading control. ($n = 3$). (B) Total cellular proteins extracted from BMMs transfected with CREB siRNAs or negative scrambled control, and stimulated with RANKL for 5 days were subjected to Western blot analysis using specific antibodies against SREBP-2 (N), CREB and NFATc1 ($n = 3$). GAPDH was used as internal loading control. (C) BMM cells overexpressing FLAG-SREBP-2 or empty vector were treated with KG-501 for 5 days for the formation of mature multinucleated osteoclasts. At the end of the experimental period, cells were fixed and stained for TRAP activity. The number and size (area) of TRAP-positive multinuclear cells with > 5 nuclei were quantified. $*p < 0.05$, $**p < 0.01$ ($n = 3$). (D) Western blot analysis of protein expression of NFATc1 and SREBP-2 using total cellular proteins extracted from cells that underwent same treatment as in C. GAPDH was used as internal loading control. ($n = 3$). Data are shown as the mean ± s.d. Scale bar, 100 μm.

correlation between SREBP-2 expression and clinical metastases in breast cancer (Fig. 5B). Furthermore, we carried out statistical analysis of the breast cancer dataset published by Van't Veer et al. in 2002 [26] and found that patients with high SREBP-2 expression exhibited significantly shorter metastasis-free survival rates than those with low SREBP-2 expression (Fig. 5C). Collectively, these results indicates that SREBP-2 may contribute to breast cancer tumorigenesis and metastasis with elevated levels of SREBP-2 being a predictor of a poor prognosis in patients with invasive breast carcinoma.

3.6. SREBP-2 inhibition suppresses migration and invasion of breast cancer cells and reduces MMPs expression

Given that SREBP-2 expression is elevated in invasive breast carcinomas, we thus investigated the effects of SREBP-2 gene knockdown on breast cancer cell migration and invasion. As shown in Fig. 5D and E, silencing of SREBP-2 gene markedly suppressed the migration and invasion of the highly metastatic human breast cancer cell line MDA-MB-231 through the transwell membrane and Matrigel respectively. Interestingly, SREBP-2 knockdown significantly reduced the expression of MMP-2 and MMP-9, the key matrix degradative proteases involved in tumor invasion and metastasis (Fig. 5F). Similarly, inhibition of SREBP-2 activation with Fatostatin or CREB signaling with KG-501, suppressed MDA-MB-231 breast cancer cell migration, invasion, and MMP-2 and MMP-9 protein expression (Fig. 5G–I). However, the direct inhibition of SREBP-2 activation with Fatostatin demonstrated a much stronger inhibitory effect than inhibition of CREB signaling with KG-501. Overexpression of SREBP-2 can again partially restore the migration and invasive potentials of MDA-MB-231 breast cancer cells as well as the expression of MMP-2 and MMP-9 (Fig. 5G–I). Interestingly, SREBP-2 knockdown demonstrated a mild inhibitory effect on breast cancer cell proliferation by promoting cellular apoptosis (Supplemental Fig. 3B–D).

3.7. Targeting SREBP-2 alleviates breast cancer cell-induced osteolytic lesions in vivo

Given the suppressive effect of SREBP-2 inhibition on MDA-MB-231 breast cancer cell migration and invasion, and osteoclast formation and bone resorption, we proposed that drug targeting of SREBP-2 as a potential therapeutic option for the treatment of breast cancer-induced osteolysis. To this end, we utilized our previously established intratibial mouse model of breast cancer-induced osteolysis to explore the effects

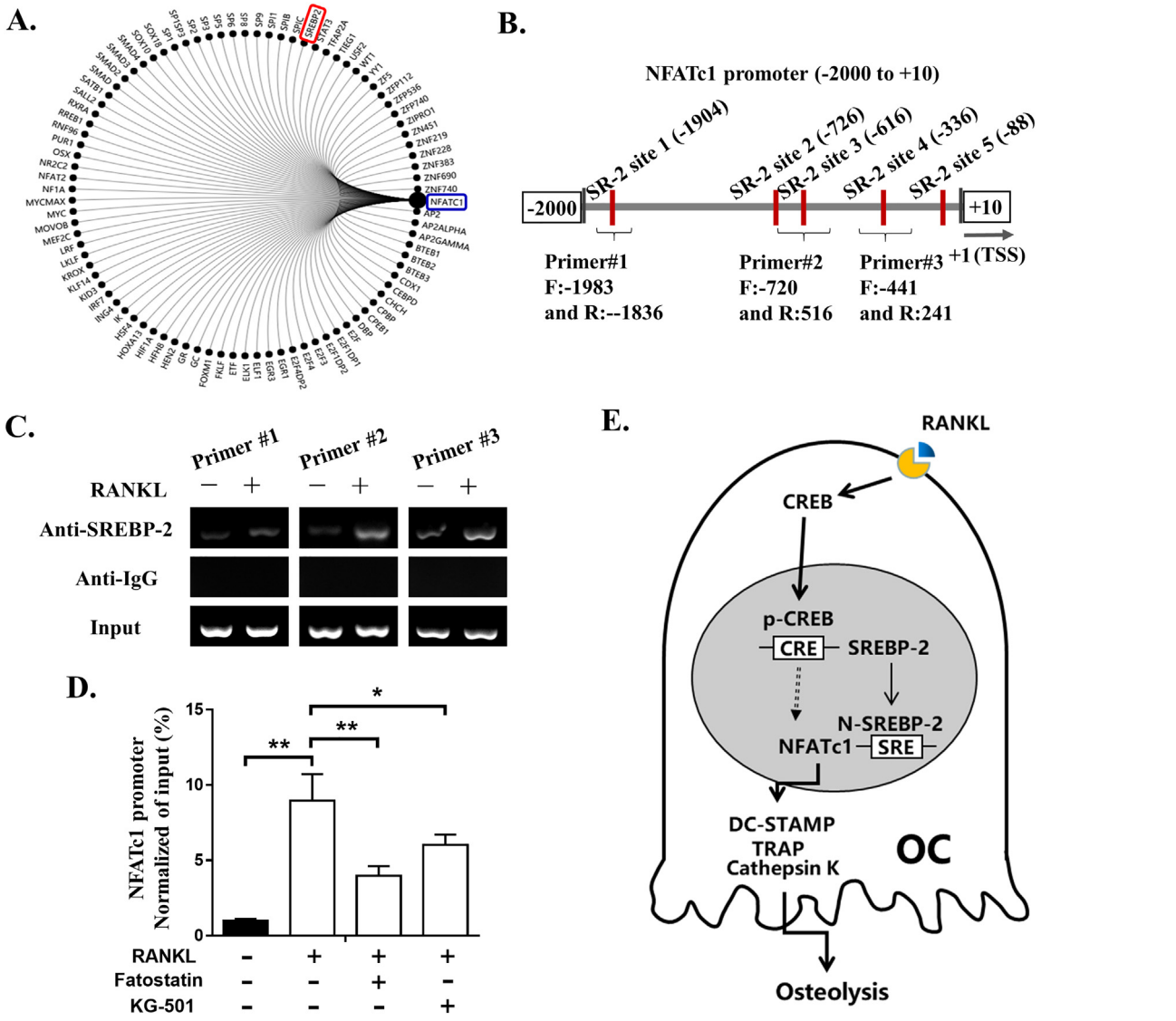

Fig. 4. SREBP-2 is a transcriptional regulator of NFATc1 Expression. (A) Transcriptional regulatory network for NFATc1 as predicted by Gene-Cloud of Biotechnology Information online server (GCBI; https://www.gcbi.com.cn). (B) Schematic of predicted putative SREBP-2 response elements and location of ChIP primers in the 2 kB promoter (−2000/+10) of NFATc1. TSS - transcriptional start site. (C) ChIP analysis of the binding of SREBP-2 to the NFATc1 promoter. BMM stimulated with RANKL for 48 h were fixed, and cross-linked protein-chromatin complexes were treated with anti-SREBP-2 or isotype matched (IgG) control antibodies. Precipitated DNA was then subjected to PCR analysis using the indicated primers directed against the 2kB NFATc1 promoter region, and products were visualized using agarose gel electrophoresis. ($n = 3$). (D) BMMs was treated with or without Fatostatin or KG-501 and stimulated with RANKL for 48 h and then subjected to ChIP analysis as described in C. The binding of SREBP-2 to the NFATc1 promoter was quantified and normalized to input control. $^{*}p < 0.05$, $^{**}p < 0.01$ ($n = 3$). (E) A hypothetical schematic representation of CREB/SREBP-2/NFATc1 signaling following RANKL stimulation. Data are shown as the mean ± s.d.

of targeting SREBP-2 with Fatostatin on osteolytic bone damage induced by breast cancer cells. As shown in the representative micro-CT images in Fig. 6A, injection of MDA-MB-231 breast cancer cells into the tibia of mice (vehicle treated group) induces extensive osteolytic bone damage when compared to sham control mice. Treatment with Fatostatin dose-dependently protected the mice against cancer cell-induced osteolysis (Fig. 6A). Fatostatin treatment prevented cancer cell-induced bone loss evidenced by higher levels of trabecular bone volume/tissue volume (Fig. 6B), trabecular number (Fig. 6C), trabecular thickness (Supplemental Fig. 4A) and Connectivity-Density (Supplemental Fig. 4B), with control levels of trabecular separation (Fig. 6D).

Histological and histomorphometric analysis shows a larger proportion of the bone is occupied by tumor tissue in the vehicle-treated group compared to Fatostatin-treated mice (Fig. 6E). Immunohistochemical staining for TRAP (Fig. 6F), SREBP2 (Fig. 6G), MMP-2 and MMP-9 (Supplemental Fig. 4A and B, respectively) in bone tissue sections further showed elevated levels of mature TRAP-positive osteoclasts lining the bone surface, and high levels of SREBP-2-positive and MMP-2/9-positive cancer cells in vehicle-treated bone tissues. The increased osteoclast number was dose-dependently suppressed following treatment with Fatostatin (Fig. 6F) and the number of SREBP-2 and MMP-2/9-positive cells were also dose-dependently reduced (Fig. 6G and Supplemental Fig. 4C–D). Collectively, these data provide evidence for the therapeutic targeting of SREBP-2 in the treatment of breast cancer-induced osteolysis.

4. Discussion

The vicious cycle established between breast cancer cells and osteoclast, can lead to cancer-induced bone destruction which seriously impacts the quality of life of patients [4,5]. Although therapeutic interventions have been developed that aims to disrupt this vicious cycle

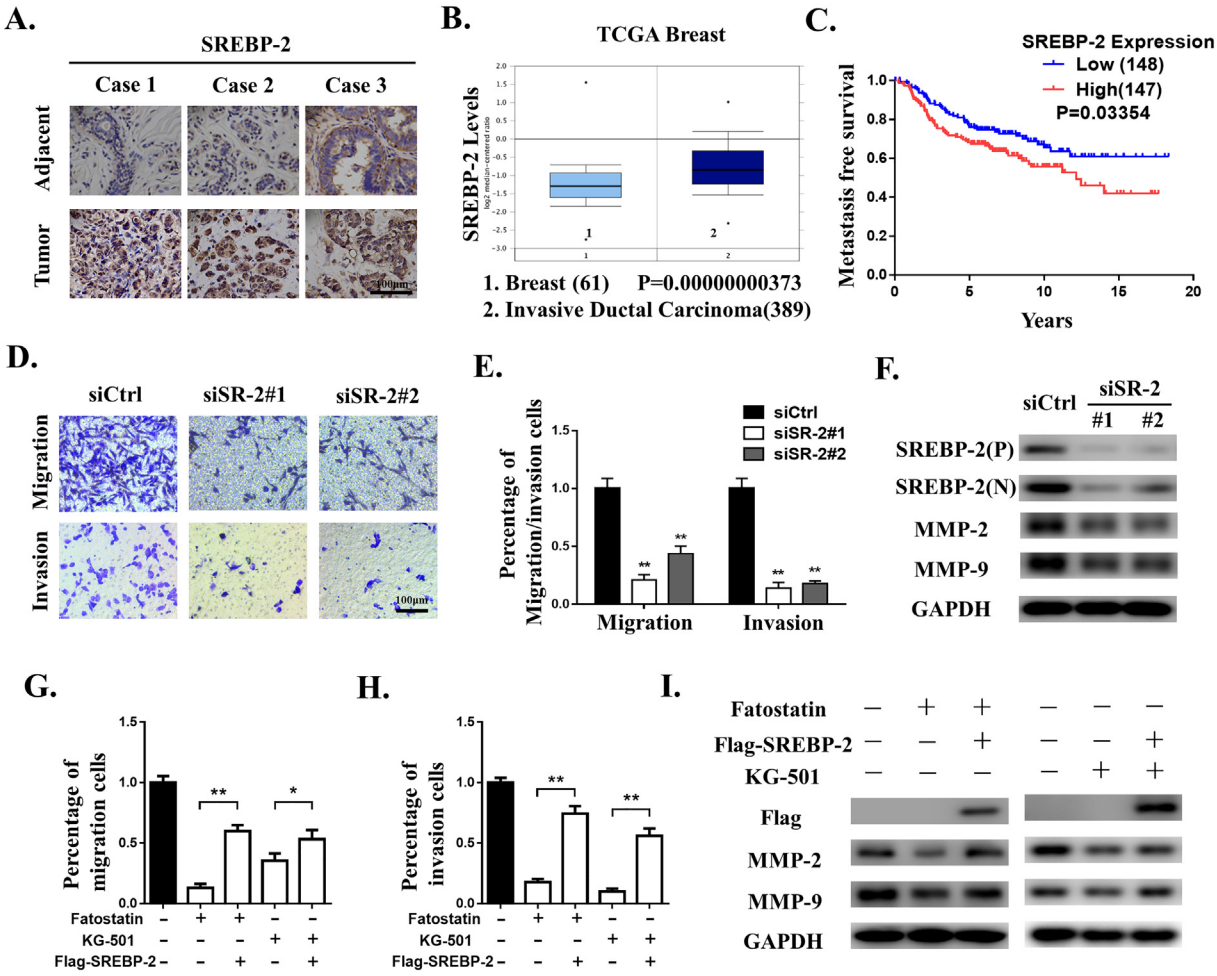

Fig. 5. SREBP-2 expression predicts poor prognosis, and promotes MDA-MB-231 cell migration and invasion. (A) Representative images of immunohistochemical staining for SREBP-2 expression in breast cancer tissue and adjacent tissues. (B) SREBP-2 expression in breast and invasive breast carcinoma samples using public available datasets from The Cancer Genome Atlas (TCGA) was analyzed using the Oncomine platform. (C) Statistical analysis of the metastasis-free survival rate of patients with breast cancer using the dataset from Van't Veer et al. [26]. (D–E) The migration and invasion potential of MDA-MB-231 human breast cancer cell transfected with SREBP-2 siRNAs or negative scrambled control was analyzed using the transwell migration assays. For the analysis of invasion potential, cells were seeded onto a Matrigel Extracellular Matrix that was prepared prior to cell seeding. $^{*}p < 0.05$, $^{**}p < 0.01$ ($n = 3$). (F) Total cellular proteins extracted from MDA-MB-231 cells transfected with SREBP-2 siRNAs or negative scrambled control were subjected to Western blot analysis using specific antibodies against SREBP-2 (N and P forms), MMP-2 and MMP-9 ($n = 3$). GAPDH was used as internal loading control. (G–H) MDA-MB-231 cells overexpressing FLAG-SREBP-2 or empty vector were treated with Fatostatin or KG-501 and the migration and invasion potential of cells were determined by transwell migration assay as described in D–E. $^{*}p < 0.05$, $^{**}p < 0.01$ ($n = 3$). (I) Total cellular lysates extracted from MDA-MB-231 cells overexpressing FLAG-SREBP-2 or empty vector and treated with Fatostatin or KG-501 were subjected to Western blot analysis using specific antibodies against MMP-2 and MMP-9 ($n = 3$). Data are shown as the mean ± s.d. Scale bar, 100 μm.

of positive regulation their efficacy remains limited [9,27]. In this study, we have shown that SREBP-2 serves as an important molecular regulator in the pathogenesis of breast cancer-induced osteolysis *in vivo*, and that therapeutic targeting of SREBP-2 may be effective for treatment option for osteolytic bone lesions in breast cancer patients.

In vitro assessments found SREBP-2 to be upregulated during osteoclast formation under the regulation of the RANKL-CREB signaling pathway. RANKL-induced activation of CREB stimulated the transcription and activation of SREBP-2, which then translocates into the nucleus where it participate in the induction of NFATc1 transcription during osteoclast formation. Suppression of SREBP2 expression by gene knockdown or CREB inhibition with KG-501, or the inhibition of SREBP-2 activation with Fatostatin, potently inhibited osteoclast formation and bone resorption. Similarly in MDA-MB-231 human breast cancer cells, CREB activation regulated the expression of SREBP-2 which was found to be involved in the transcriptional regulation of MMP-2 and MMP-9 expression. Furthermore, elevated levels of SREBP-2 expression was highly correlated with the invasive metastatic breast carcinomas and was found to be a predictor of poor prognosis for breast cancer patients. Thus our data suggested that SREBP-2 is intimately involved in the vicious cycle of breast cancer-induced osteolysis by promoting breast cancer metastasis and inducing osteoclast differentiation and bone resorption.

Abnormal and elevated activation of osteoclast formation and function in breast cancer patients with bone metastasis is one of the major causes of bone osteolysis that impacts the quality of life of the patients [3,28]. Activation of RANK on BMMs by its ligand RANKL, leads to the expression of osteoclast-related genes that are involved in promoting osteoclast lineage commitment, precursor cell fusion, and mature osteoclast bone resorption [13,15]. SREBP-2 is well study in the context of regulating cholesterol homeostasis by transcriptionally activating its target genes [29]. Furthermore, previous studies have demonstrated that cholesterol homeostasis is strongly involved in osteoclast formation and function [30,31]. Additionally, a genome-wide DNase-seq analysis study performed by Inoue and colleagues [17] found SREBP-2 as a potential novel transcriptional regulator of

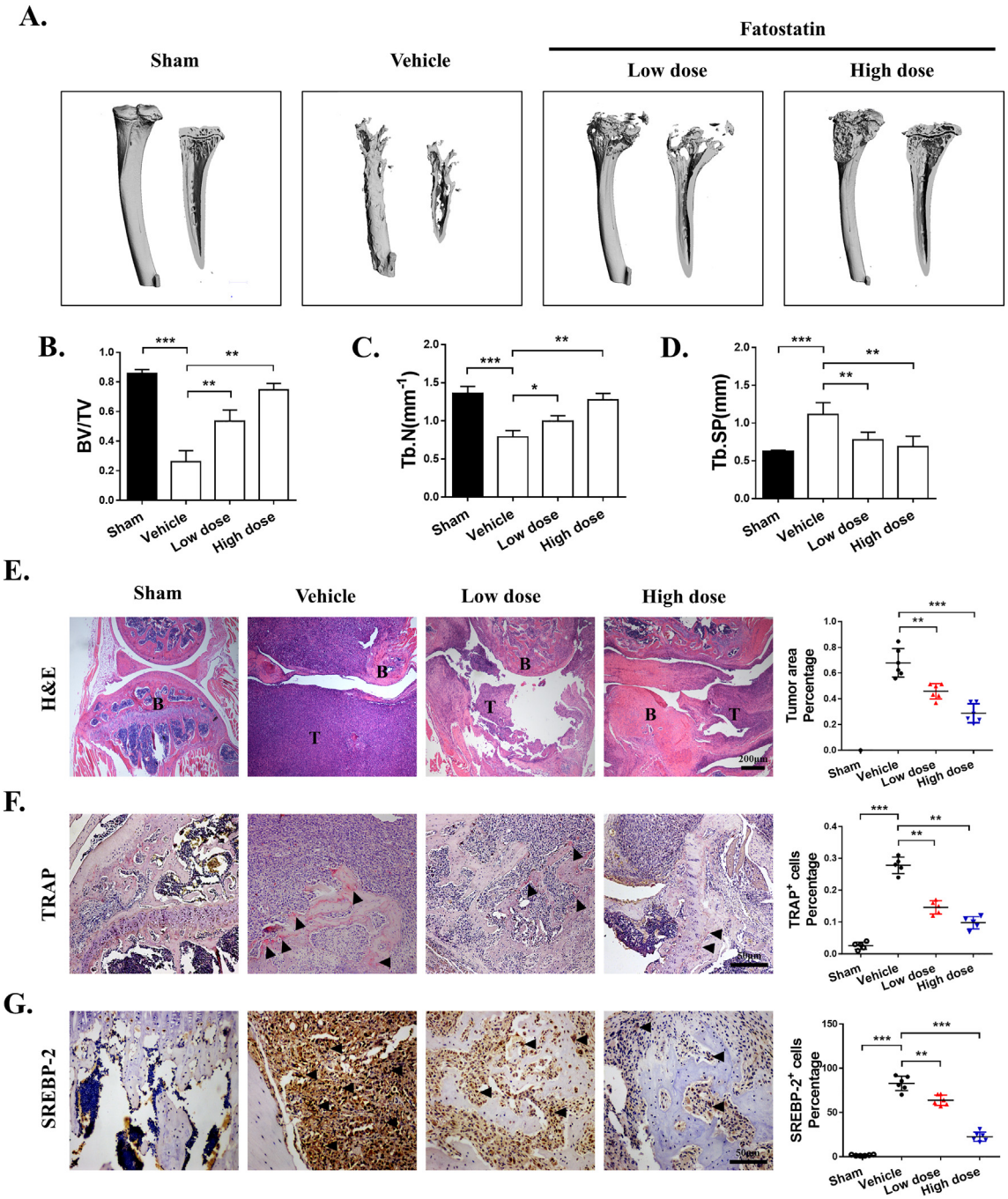

Fig. 6. Targeting SREBP-2 alleviates breast cancer-induced osteolytic lesions *in vivo*. (A) MDA-MB-231 cells were injected directly into the tibiae plateau, and the tibiae was analyzed by micro-CT after 28 days. Three-dimensional reconstructed images are presented following the resection of the tibial bone ($n = 6$). (B–D) The trabecular bone volume to tissue volume (BV/TV) ratio, trabecular number (Tb.N), and trabecular separation (Tb.Sp) of each sample was quantified. $^{*}p < 0.05$, $^{**}p < 0.01$, $^{***}p < 0.001$ ($n = 6$). (E–G) Tibiae sections were fixed, decalcified, dehydrated, sectioned and then stained with H&E, for TRAP, and for SREBP-2. The tumor size, number of TRAP-positive osteoclasts, and number of SREBP-2-positive cells were quantified. $^{*}p < 0.05$, $^{**}p < 0.01$, $^{***}p < 0.001$ ($n = 6$). Data are shown as the mean ± s.d. Scale bar in E 200 μm. Scale bar in F, G 100 μm.

osteoclast differentiation [17]. Our study provided further evidence that SREBP-2 is novel regulator that is robustly induced in osteoclasts with SREBP-2 inhibition suppressing RANKL-induced osteoclast formation and bone resorption and NFATc1 induction.

The CREB transcriptional factor and its associated signaling cascade plays an important role in osteoclast formation [32]. CREB binds to cAMP-response elements (CRE) in the promoter of target genes thereby regulating the transcriptional expression of these genes [33]. We found CREB to be highly induced during osteoclast formation and its expression precedes that of SREBP-2 induction. Gene knockdown of CREB gene expression significantly reduced the expression of SREBP-2 and NFATc1, which was correlated with the inhibition of osteoclast differentiation. Previous study by Li and colleagues showed that the promoter region of SREBP-2 contains a CRE half-site (TGACGTAA) that can be recognized by CREB [34] and based on this information and our data we believe that SREBP-2 gene expression during osteoclast formation is under the regulatory control of RANKL-CREB signaling axis.

During osteoclastogenesis, RANKL-induced NFATc1 induction is indispensable for osteoclast development [35]. Embryonic stem cells lacking NFATc1 fails to differentiate into osteoclasts [36] whereas

ectopic expression of a constitutively active NFATc1 induces osteoclast formation in the absence of RANKL [37]. Using online-based transcriptional element search software we identified a number of putative SREBP-2 response elements (SRE) in the NFATc1 2kB promoter. Furthermore, ChIP analysis confirmed binding of SREBP-2 to these putative SRE in the NFATc1 promoter. This results provides an explanation as to why the suppression of SREBP-2 gene expression or activity reduced NFATc1 expression and osteoclast formation.

SREBP-2 has recently been found to exert multiple effects in various tumors [38,39]. Importantly, cholesterol-lowering medication have been reported to play a role in preventing breast cancer recurrence [40] suggesting a role for SREBP-2 in breast cancer tumorigenesis. In our study, we found SREBP-2 to be highly expressed in breast cancer tissue samples and bioinformatics analysis of TCGA datasets found that high SREBP-2 expression was correlated with invasive breast carcinoma and predictive of a poor prognosis. We further verified this correlation by carrying out *in vitro* migration and invasion assays. Suppression of SREBP-2 either by gene knockdown or inhibition of SREBP-2 activation, was found to potently restrain the migration and invasion of human MDA-MB-231 breast cancer cells, the cytological fundament of tumor metastasis.

MMPs are key proteases involved in tumor invasion and metastasis and are considered to be important in the bone metastatic process [41]. Over 20 members make up the MMP family and they can collectively degrade all components of the extracellular matrix [41]. Previous studies demonstrated that MMP-2 and MMP-9 as important degradative proteases involved in mediating breast cancer cell invasion and metastasis [42,43]. Interestingly, knockdown of SREBP-2 gene expression or inhibiting the activation of SREBP-2 with Fatostatin, reduced the expression of both MMP-2 and MMP-9. Furthermore, inhibition of CREB signaling was also found to inhibit cell migration, invasion, and MMP-2/9 expression suggesting that the CREB signaling pathway plays a universal role in regulating SREBP-2 expression and thus a viable therapeutic target for breast cancer-induced osteolysis.

The underlying mechanism of breast cancer metastasis from the primary tumor to the bone is a very complex and remains to be fully elucidated [3]. The contribution of the primary tumor microenvironment to malignant progression plays a very important role [44–46]. Our animal model was designed with breast cancer-induced bone destruction as the final outcome and not as a model for the malignant metastasis of the primary mammary tissues to the distant skeletal system. We recognize this as a limitation of the study and therefore it is impossible to fully assess the direct effect of SREBP-2 inhibition therapy on breast cancer metastases to bone. None-the-less, we found that targeted inhibition of SREBP-2 with Fatostatin can protect against breast cancer-induced osteolysis by inhibiting osteoclast formation and activity. Furthermore, tumor size in the bone was also significantly reduced with lower expressions of SREBP-2 and MMPs.

In conclusion, our study has provided evidence that SREBP-2 as a novel and important transcription factor regulating osteoclast formation and function, and in breast cancer cell migration and invasion. Agents targeting SREBP-2 may offer therapeutic benefits by countering bone destruction induced by breast cancer bone metastases.

Supplementary data to this article can be found online at https://doi.org/10.1016/j.bbadis.2018.10.026.

Transparency document

The Transparency document associated with this article can be found, in online version.

Acknowledgements

The authors would like to thank all the staff in the Department of Orthopaedics, Sir Run Run Shaw Hospital, School of Medicine, Zhejiang University for their support. The authors are grateful to all staffs who contributed to this study.

Funding

This work was supported by the National Natural Science Foundation of China (81772373; 81572167; 81772387; 81472064), National Key R&D Program of China (No. 2018YFC1105200), the Key Research and Development Plan in Zhejiang province (No. 2018C03060), and the Health Department of Zhejiang Province (grant number 2017KY024).

Contributions

JZW, XZA, QA, and FSW conceived and designed the experiments. JZW, XZA, XWB, and ZXD performed the experiments. JZW, XZA, SXW, HB, and TP conducted the animal study. JZW, XZA, XWB, WGL, and QA analyzed the data. QA and FSW supervised the experiments. JZW, XZA, and XWB drafted the manuscript. SSY, QA, and FSW revised the manuscript. All authors approved the final version of the manuscript.

Conflict of interest statement

All authors read and approved the final version of the manuscript, and the authors have no conflict interest to declare.

References

[1] K.M. Bussard, C.V. Gay, A.M. Mastro, The bone microenvironment in metastasis; what is special about bone? Cancer Metastasis Rev. 27 (2008) 41–55.
[2] A. Kommalapati, S.H. Tella, M.A. Esquivel, R. Correa, Evaluation and management of skeletal disease in cancer care, Crit. Rev. Oncol. Hematol. 120 (2017) 217–226.
[3] G.D. Roodman, Mechanisms of bone metastasis, N. Engl. J. Med. 350 (2004) 1655–1664.
[4] T. Yoneda, M. Hiasa, Y. Nagata, T. Okui, F. White, Contribution of acidic extracellular microenvironment of cancer-colonized bone to bone pain, Biochim. Biophys. Acta 1848 (2015) 2677–2684.
[5] A. Bellanger, C.F. Donini, J.A. Vendrell, J. Lavaud, I. Machuca-Gayet, M. Ruel, J. Vollaire, E. Grisard, B. Gyorffy, I. Bieche, O. Peyruchaud, J.L. Coll, I. Treilleux, V. Maguer-Satta, V. Josserand, P.A. Cohen, The critical role of the ZNF217 oncogene in promoting breast cancer metastasis to the bone, J. Pathol. 242 (2017) 73–89.
[6] M.L. Blake, M. Tometsko, R. Miller, J.C. Jones, W.C. Dougall, RANK expression on breast cancer cells promotes skeletal metastasis, Clin. Exp. Metastasis 31 (2014) 233–245.
[7] G.R. Mundy, Metastasis to bone: causes, consequences and therapeutic opportunities, Nat. Rev. Cancer 2 (2002) 584–593.
[8] M. Futakuchi, K. Fukamachi, M. Suzui, Heterogeneity of tumor cells in the bone microenvironment: mechanisms and therapeutic targets for bone metastasis of prostate or breast cancer, Adv. Drug Deliv. Rev. 99 ((2016) 206–211.
[9] M.T. Drake, S.C. Cremers, Bisphosphonate therapeutics in bone disease: the hard and soft data on osteoclast inhibition, Mol. Interv. 10 (2010) 141–152.
[10] A. Lipton, I. Jacobs, Denosumab: benefits of RANK ligand inhibition in cancer patients, Curr. Opin. Support Palliat. Care 5 (2011) 258–264.
[11] C. Reyes, M. Hitz, D. Prieto-Alhambra, B. Abrahamsen, Risks and benefits of bisphosphonate therapies, J. Cell. Biochem. 117 (2016) 20–28.
[12] J.H. Park, N.K. Lee, S.Y. Lee, Current understanding of RANK signaling in osteoclast differentiation and maturation, Mol. Cells 40 (2017) 706–713.
[13] W.J. Boyle, W.S. Simonet, D.L. Lacey, Osteoclast differentiation and activation, Nature 423 (2003) 337–342.
[14] W. Chen, G. Zhu, J. Tang, H.D. Zhou, Y.P. Li, C/ebpalpha controls osteoclast terminal differentiation, activation, function, and postnatal bone homeostasis through direct regulation of Nfatc1, J. Pathol. 244 (2018) 271–282.
[15] S.L. Teitelbaum, Bone resorption by osteoclasts, Science 289 (2000) 1504–1508.
[16] H. Shimano, R. Sato, SREBP-regulated lipid metabolism: convergent physiology - divergent pathophysiology, Nat. Rev. Endocrinol. 13 (2017) 710–730.
[17] K. Inoue, Y. Imai, Identification of novel transcription factors in osteoclast differentiation using genome-wide analysis of open chromatin determined by DNase-seq, J. Bone Miner. Res. 29 (2014) 1823–1832.
[18] K. Inoue, Y. Imai, Fatostatin, an SREBP inhibitor, prevented RANKL-induced bone loss by suppression of osteoclast differentiation, Biochim. Biophys. Acta 1852 (2015) 2432–2441.
[19] X. Li, Y.T. Chen, P. Hu, W.C. Huang, Fatostatin displays high antitumor activity in prostate cancer by blocking SREBP-regulated metabolic pathways and androgen receptor signaling, Mol. Cancer Ther. 13 (2014) 855–866.
[20] M. Chen, J. Zhang, K. Sampieri, J.G. Clohessy, L. Mendez, E. Gonzalez-Billalabeitia, X.S. Liu, Y.R. Lee, J. Fung, J.M. Katon, A.V. Menon, K.A. Webster, C. Ng, M.D. Palumbieri, M.S. Diolombi, S.B. Breitkopf, J. Teruya-Feldstein, S. Signoretti,

R.T. Bronson, J.M. Asara, M. Castillo-Martin, C. Cordon-Cardo, P.P. Pandolfi, An aberrant SREBP-dependent lipogenic program promotes metastatic prostate cancer, Nat. Genet. 50 (2018) 206–218.
[21] A.A. Gholkar, K. Cheung, K.J. Williams, Y.C. Lo, S.A. Hamideh, C. Nnebe, C. Khuu, S.J. Bensinger, J.Z. Torres, Fatostatin inhibits cancer cell proliferation by affecting mitotic microtubule spindle assembly and cell division, J. Biol. Chem. 291 (2016) 17001–17008.
[22] Z. Xie, H. Yu, X. Sun, P. Tang, Z. Jie, S. Chen, J. Wang, A. Qin, S. Fan, A novel diterpenoid suppresses osteoclastogenesis and promotes osteogenesis by inhibiting Ifrd1-mediated and IkappaBalpha-mediated p65 nuclear translocation, J. Bone Miner. Res. 33 (2018) 667–678.
[23] Z. Jie, Z. Xie, X. Zhao, X. Sun, H. Yu, X. Pan, S. Shen, A. Qin, X. Fang, S. Fan, Glabridin inhibits osteosarcoma migration and invasion via blocking the p38- and JNK-mediated CREB-AP1 complexes formation, J. Cell. Physiol. (2018), https://doi.org/10.1002/jcp.27171.
[24] Q. Wang, J. Mo, C. Zhao, K. Huang, M. Feng, W. He, J. Wang, S. Chen, Z. Xie, J. Ma, S. Fan, Raddeanin A suppresses breast cancer-associated osteolysis through inhibiting osteoclasts and breast cancer cells, Cell Death Dis. 9 (2018) 376.
[25] H. Qiao, T.Y. Wang, Z.F. Yu, X.G. Han, X.Q. Liu, Y.G. Wang, Q.M. Fan, A. Qin, T.T. Tang, Structural simulation of adenosine phosphate via plumbagin and zoledronic acid competitively targets JNK/Erk to synergistically attenuate osteoclastogenesis in a breast cancer model, Cell Death Dis. 7 (2016) e2094.
[26] L.J. van't Veer, H. Dai, M.J. van de Vijver, Y.D. He, A.A. Hart, M. Mao, H.L. Peterse, K. van der Kooy, M.J. Marton, A.T. Witteveen, G.J. Schreiber, R.M. Kerkhoven, C. Roberts, P.S. Linsley, R. Bernards, S.H. Friend, Gene expression profiling predicts clinical outcome of breast cancer, Nature 415 (2002) 530–536.
[27] S. Koob, M. Kehrer, A. Strauss, V. Janzen, D.C. Wirtz, J. Schmolders, Bone metastases - pathophysiology, diagnostic testing and therapy (part 1), Z. Orthop. Unfall 155 (2017) 716–726.
[28] A. Maurizi, N. Rucci, The osteoclast in bone metastasis: player and target, Cancers (Basel) 10 (2018).
[29] G. Musso, R. Gambino, M. Cassader, Cholesterol metabolism and the pathogenesis of non-alcoholic steatohepatitis, Prog. Lipid Res. 52 (2013) 175–191.
[30] N. Hada, M. Okayasu, J. Ito, M. Nakayachi, C. Hayashida, T. Kaneda, N. Uchida, T. Muramatsu, C. Koike, M. Masuhara, T. Sato, Y. Hakeda, Receptor activator of NF-kappaB ligand-dependent expression of caveolin-1 in osteoclast precursors, and high dependency of osteoclastogenesis on exogenous lipoprotein, Bone 50 (2012) 226–236.
[31] E. Luegmayr, H. Glantschnig, G.A. Wesolowski, M.A. Gentile, J.E. Fisher, G.A. Rodan, A.A. Reszka, Osteoclast formation, survival and morphology are highly dependent on exogenous cholesterol/lipoproteins, Cell Death Differ. 11 (Suppl. 1) (2004) S108–S118.
[32] K. Sato, A. Suematsu, T. Nakashima, S. Takemoto-Kimura, K. Aoki, Y. Morishita, H. Asahara, K. Ohya, A. Yamaguchi, T. Takai, T. Kodama, T.A. Chatila, H. Bito, H. Takayanagi, Regulation of osteoclast differentiation and function by the CaMK-CREB pathway, Nat. Med. 12 (2006) 1410–1416.
[33] B. Mayr, M. Montminy, Transcriptional regulation by the phosphorylation-dependent factor CREB, Nat. Rev. Mol. Cell. Biol. 2 (2001) 599–609.
[34] Y. Li, Y. Song, M. Zhao, Y. Guo, C. Yu, W. Chen, S. Shao, C. Xu, X. Zhou, L. Zhao, Z. Zhang, T. Bo, Y. Xia, C.G. Proud, X. Wang, L. Wang, J. Zhao, L. Gao, A novel role for CRTC2 in hepatic cholesterol synthesis through SREBP-2, Hepatology 66 (2017) 481–497.
[35] J. Lorenzo, The many ways of osteoclast activation, J. Clin. Invest. 127 (2017) 2530–2532.
[36] M. Asagiri, H. Takayanagi, The molecular understanding of osteoclast differentiation, Bone 40 (2007) 251–264.
[37] H. Takayanagi, S. Kim, T. Koga, H. Nishina, M. Isshiki, H. Yoshida, A. Saiura, M. Isobe, T. Yokochi, J. Inoue, E.F. Wagner, T.W. Mak, T. Kodama, T. Taniguchi, Induction and activation of the transcription factor NFATc1 (NFAT2) integrate RANKL signaling in terminal differentiation of osteoclasts, Dev. Cell 3 (2002) 889–901.
[38] A. Kondo, S. Yamamoto, R. Nakaki, T. Shimamura, T. Hamakubo, J. Sakai, T. Kodama, T. Yoshida, H. Aburatani, T. Osawa, Extracellular acidic pH activates the sterol regulatory element-binding protein 2 to promote tumor progression, Cell Rep. 18 (2017) 2228–2242.
[39] T. Porstmann, B. Griffiths, Y.L. Chung, O. Delpuech, J.R. Griffiths, J. Downward, A. Schulze, PKB/Akt induces transcription of enzymes involved in cholesterol and fatty acid biosynthesis via activation of SREBP, Oncogene 24 (2005) 6465–6481.
[40] S. Borgquist, A. Giobbie-Hurder, T.P. Ahern, J.E. Garber, M. Colleoni, I. Lang, M. Debled, B. Ejlertsen, R. von Moos, I. Smith, A.S. Coates, A. Goldhirsch, M. Rabaglio, K.N. Price, R.D. Gelber, M.M. Regan, B. Thurlimann, Cholesterol, cholesterol-lowering medication use, and breast cancer outcome in the BIG 1-98 study, J. Clin. Oncol. 35 (2017) 1179–1188.
[41] C.M. Overall, C. Lopez-Otin, Strategies for MMP inhibition in cancer: innovations for the post-trial era, Nat. Rev. Cancer 2 (2002) 657–672.
[42] H.S. Azzam, G. Arand, M.E. Lippman, E.W. Thompson, Association of MMP-2 activation potential with metastatic progression in human breast cancer cell lines independent of MMP-2 production, J. Natl. Cancer Inst. 85 (1993) 1758–1764.
[43] X.Y. Bai, S. Li, M. Wang, X. Li, Y. Yang, Z. Xu, B. Li, Y. Li, K. Xia, H. Chen, H. Wu, Kruppel-like factor 9 down-regulates matrix metalloproteinase 9 transcription and suppresses human breast cancer invasion, Cancer Lett. 412 (2018) 224–235.
[44] S. Mittal, N.J. Brown, I. Holen, The breast tumor microenvironment: role in cancer development, progression and response to therapy, Expert. Rev. Mol. Diagn. 18 (2018) 227–243.
[45] P.S. Steeg, Tumor metastasis: mechanistic insights and clinical challenges, Nat. Med. 12 (2006) 895–904.
[46] A.F. Chambers, A.C. Groom, I.C. MacDonald, Dissemination and growth of cancer cells in metastatic sites, Nat. Rev. Cancer 2 (2002) 563–572.